Focal epilepsy modulates vesicular positioning at cortical synapses

Eleonora Vannini[1,2,3], Laura Restani[1], Marialaura Dilillo[4], Liam McDonnell[4], Matteo Caleo[1,5,#], Vincenzo Marra[2,*,#]*

[1] Neuroscience Institute, National Research Council (CNR), via G. Moruzzi 1, 56124 Pisa, Italy
[2] Department of Neuroscience, Psychology and Behaviour, University of Leicester, Leicester LE1 7RH, United Kingdom
[3] Fondazione Umberto Veronesi, Piazza Velasca 5, 20122 Milan, Italy
[4] Fondazione Pisana per la Scienza Onlus (FPS), via Ferruccio Giovannini 13, San Giuliano Terme, 56017 Pisa, Italy
[5] Department of Biomedical Sciences, University of Padua, via G. Colombo 3, 35121 Padua, Italy

Running Title: Vesicular dynamics changes at nanoscale levels in epilepsy
Keywords: synaptic vesicles; hyperexcitability; visual cortex; homeostatic plasticity; epilepsy; visual processing; carboxypeptidase E, tetanus neurotoxin
*Corresponding authors: Dr Eleonora Vannini, Email e.vannini@in.cnr.it; Dr Vincenzo Marra, Email vm120@le.ac.uk
#Equal contribution

Abstract

Neuronal networks' hyperexcitability often results from an unbalance between excitatory and inhibitory neurotransmission; however, underlying synaptic alterations leading to this condition remains poorly understood. Here, we assess synaptic changes in the visual cortex of epileptic tetanus neurotoxin-injected mice. Using an ultrastructural measure of synaptic activity, we quantified functional differences at excitatory and inhibitory synapses. We found homeostatic changes in hyperexcitable networks, expressed as an early onset lengthening of active zones at inhibitory synapses followed by spatial reorganization of recycled vesicles at excitatory synapses. A proteomic analysis of synaptic content revealed an upregulation of Carboxypeptidase E (CPE) following Tetanus NeuroToxin (TeNT) injection. Remarkably, inhibition of CPE rapidly decreased network discharges *in vivo*. These analyses reveal a complex landscape of homeostatic changes affecting the epileptic synaptic release machinery, differentially at inhibitory and excitatory terminals. Our study unveil homeostatic presynaptic mechanisms which may impact release timing rather than synaptic strength.

Introduction

The correct functioning of neuronal networks requires precise modulation of excitatory and inhibitory activity. When network activity is tipped out of balance, a number of cellular processes take place to re-establish its normal function (Turrigiano, 2012). These cellular processes underlying homeostatic plasticity can affect cellular activity and synaptic output (Wefelmeyer, Puhl and Burrone, 2016). Following a perturbation, neurons attempt to restore their baseline firing rates and dynamic range by regulating their intrinsic excitability, presynaptic probability of neurotransmitter release and neurotransmitter receptor expression (Davis and Müller, 2015). Homeostatically induced scaling-up has been studied in great detail. Indeed, a number of reports in cultured neurons have demonstrated that homeostatic scaling-down can affect excitability and synaptic strength (Grubb and Burrone, 2010). Other studies have demonstrated scaling-down *in vivo* (Gonzalez-Islas and Wenner, 2006; Ibata, Sun and Turrigiano, 2008; Tatavarty, Sun and Turrigiano, 2013; Gonzalez-Islas *et al.*, 2016; Diering *et al.*, 2017). One particularly useful model that has provided invaluable information on the time course of cortical re-organization after sensory lack is monocular deprivation (MD), which results in temporary reduction of activity in one of the two eyes (Desai *et*

al., 2002; De Paola *et al.*, 2006; Maffei *et al.*, 2006; Stettler *et al.*, 2006; Maffei and Turrigiano, 2008; Restani *et al.*, 2009; Yamahachi *et al.*, 2009; Keck *et al.*, 2011). Experiments on this paradigmatic model have shown a homeostatic enhancement of the cortical responses elicited by the occluded eye after brief MD, in rodents and in humans (Mrsic-Flogel *et al.*, 2007; Lunghi, Burr and Morrone, 2011; Hengen *et al.*, 2013; Binda *et al.*, 2018). A reduction in synaptic inhibition has been hypothesized to contribute to these homeostatic changes (Barnes *et al.*, 2015; Lunghi *et al.*, 2015; Erchova *et al.*, 2017). However, much less is known about the mechanisms of scaling-down activity as a consequence of a pathological, system-level perturbation *in vivo* (Turrigiano, 2008, 2012; González *et al.*, 2019).

Here, we took advantage of a well-characterised model of focal epilepsy in the visual cortex (Mainardi *et al.*, 2012; Chang *et al.*, 2018) to investigate synaptic changes in hyperexcitable networks. Tetanus neurotoxin (TeNT) is a metalloprotease that cleaves the synaptic protein VAMP/synaptobrevin, leading to the establishment of a focal cortical epilepsy (Nilsen, Walker and Cock, 2005; Mainardi *et al.*, 2012; Vannini *et al.*, 2016; Snowball *et al.*, 2019). Hyperexcitability is detectable in TeNT-treated animals both during and after the time window of action of the toxin (respectively named acute and chronic phase, 10 and 45 days after toxin injection). Both epileptic groups exhibit spontaneous seizures, altered visual processing and structural modifications of dendritic spines and branches (Mainardi *et al.*, 2012; Vannini *et al.*, 2016). A few studies have shown homeostatic plastic events in animal models of epilepsy, including changes in the expression of specific ion channels (i.e. Potassium, Sodium, Calcium) (Meier *et al.*, 2014; Swann and Rho, 2014; Ma *et al.*, 2019). Here we used FM1-43FX and activity-dependent labelling of synaptic vesicles to simultaneously investigate function and ultrastructure of excitatory and inhibitory terminals in both acute and chronic phases of TeNT-induced epilepsy. We combined this approach with an unbiased measure of proteins content in the two phases of hyperexcitability, isolating synaptosomes at different time points after TeNT injection. Finally, we assessed the impact of inhibiting Carboxypeptidase E (CPE), upregulated in epileptic mice, using electrophysiological recordings.

Results

Ultrastructural investigation of synaptic vesicle function in hyperexcitable networks

Our studies included three groups of C57BL/6 mice: a control group injected intracranially with vehicle (Control) in the primary visual cortex (V1), an Acute epileptic group tested 10 days after TeNT injection in V1 and a Chronic epileptic group tested 45 days after TeNT injection in V1. Synaptic vesicles from 3 animals in each of these groups were labelled by infusing FM1-43FX in the visual cortex while presenting a series of mild visual stimuli (**Fig. 1A**). After fixation, photoconversion and processing for electron microscopy, we were able to label individual vesicles at excitatory (asymmetrical) and inhibitory (symmetrical) synapses (**Fig. 1A**). This approach allowed us to identify individual synaptic vesicles, released and recycled in the presence of FM1-43FX, as having an electron dense lumen, while non-released vesicles present a clear lumen and a darker membrane (Marra et al., 2012). First, we investigated the length of the active zone as a readout of synaptic activity independent of our labelling protocol (Harris and Weinberg, 2012). Surprisingly, we found an increase in the length of inhibitory synapses' active zone in the acute phase (**Fig. 1B**), normally associated with increased release. However, the released fraction of inhibitory vesicles (number of released vesicles over total number of vesicles) is reduced in animals injected with TeNT (**Fig. 1C**), shown to preferentially impair inhibitory release (Schiavo, Matteoli and Montecucco, 2000). No

differences in active zone length and released fraction of excitatory vesicles were found at excitatory synapses (**Fig. 1B, 1C**). These data suggest an early, homeostatic lengthening of inhibitory active zones in response to TeNT-induced impairment in release - which is lost at chronic stages of pathology.

Changes in docking and positioning of activated vesicles at excitatory synapses in chronic epilepsy

After quantifying direct and indirect measures of vesicular release, we examined the spatial distribution of released and non-released vesicles within presynaptic terminals. We started by analysing the released fraction in the docked population and non-docked population of vesicles. As described before for excitatory synapses (Marra et al., 2012), the Control group showed a higher released fraction in the docked population, similar results are found in the Acute group. Conversely, in the Chronic group the released fraction was higher in the non-docked population at excitatory synapses (**Fig. 2A**). We also report that inhibitory synapses have a higher released fraction in the docked population, which does not seem to be affected by the induction of epilepsy (**Fig. 2A**). To gain insight on the effect observed at excitatory synapses of the Chronic group we compared the distance of released and non-released vesicles from the active zone (**Fig. 2B**). We reason that if the effect is specific to the ability of released vesicles to dock, their position within the terminal should not be affected. We examined the cumulative fraction of the distance of released and non-released vesicles from their closest point on the active zone. At excitatory synapses, in Control and Acute groups the released vesicle population are closer to the active zone compare to the non-released population. However in the Chronic group released excitatory vesicles do not show a bias towards the active zone observed in the other groups (**Fig. 2B**). At inhibitory synapses, the distances of vesicular populations to the active zone has a different pattern, with no difference between released and non-released population in Control and Acute groups and a bias of released vesicles towards the active zone in the Chronic groups (**Fig. 2B**). While potentially interesting, the results observed at inhibitory synapses may be confounded by the change in active zone length described in the acute phase (**Fig. 1B**). As a visual representation of the distribution of released vesicles at excitatory and inhibitory across the three conditions, we generated 2D histograms of the distribution of released vesicles within spatially normalised terminals with the centre of the active zone at the origin of the X axis (**Fig. 2C**). This representation shows a clear broadening of the distribution of released excitatory vesicles in the chronic phase.

Upregulation of synaptic proteins involved in vesicle positioning in Acute and Chronic phase

To understand molecular changes in hyperexcitable networks, we performed an in-depth proteomic analysis of visual cortex synaptosomes. The expression profile of 1991 synaptic proteins extracted from animals in the acute and chronic phase of epilepsy was compared with controls. Using a fold change cut-off of 0.6, we found a total of 70 regulated proteins (51 proteins upregulated and 19 downregulated; **Fig. 3A, 3B**). As expected following TeNT injection, the Acute group showed a significant downregulation of VAMP1 and VAMP2 (Mainardi *et al.*, 2012; Vannini *et al.*, 2016). Interestingly, a few synaptic proteins remained upregulated at both stages of epilepsy, suggesting that one single TeNT injection is sufficient to induce persistent plastic changes. Proteins involved in synthesis of regulatory peptides, WNT pathway, immune response and membrane-trafficking were upregulated in hyperexcitable mice (i.e. Dickhopf related protein 3, Complement component 1q, Synaptotagmin 5, Semaphorin 4a, Carboxypeptidase E, Chromogranin B). The upregulation of neuropeptides was in line with previous reports (Vezzani and Sperk, 2004; Kovac and

Walker, 2013; Clynen et al., 2014; Dobolyi et al., 2014; Nikitidou Ledri et al., 2016). These data prompted us to quantify the density of Dense Core Vesicles (DCV) in synaptic terminals. To this aim, we performed electron microscopy on samples collected from control and experimental animals, but we found no difference in the number of DCV in the three conditions (**Fig. 3C**). Given the lack of a detectable change in DCV, we focused our study on Carboxypeptidase E (CPE), known for its effect on synaptic vesicles distribution. CPE knock out animals show an increased distance between vesicle clusters and the active zone(Park, Cawley and Loh, 2008; Lou *et al.*, 2010). Consistent with CPE upregulation, we found a tightening of synaptic vesicle clusters at excitatory synapses in the Acute and Chronic groups and at inhibitory terminals in the Acute group (**Fig. 3D**). We limited our analysis to non-released vesicles whose position is less likely to have been affected by recent recycling.

Acute Carboxypeptidase E inhibition reduces seizure activity in epileptic mice

Based on the indication that CPE upregulation may influence vesicular positioning, we performed *in vivo* electrophysiological recordings in acute epileptic mice before and after pharmacological inhibition of CPE. We performed local field potential (LFP) recordings using a 16-channel silicon probe, spanning the whole cortical thickness in awake epileptic mice. Recording channels were divided in superficial (5 channels), intermediate (6 channels) and deep (5 channels) in reference to their position in the primary visual cortex. After baseline recording of seizures, we topically administered on the visual cortex GEMSA, a CPE inhibitor (**Fig. 4A, 4B**). The recording sessions following GEMSA administration showed a significant reduction in coastline and a non-significant reduction in spike numbers on all 3 channel groups (**Fig. 4C, 4D**), indicating that CPE inhibition reduces indicators of seizure activity in epileptic mice.

Discussion

This study provides new insight on functional and ultrastructural synaptic changes in hyperexcitable neuronal networks. Using a well-established model of epilepsy, we observed differential regulation of vesicular positioning and active zone size at excitatory and inhibitory synapses (**Fig. 1, 2**). We identified a homeostatic increase in active zone length at inhibitory synapses after GABAergic release, known to be impaired by TeNT (Schiavo, Matteoli and Montecucco, 2000; Ferecskó *et al.*, 2015). These early changes at inhibitory synapses are consistent with previous observations made in the acute phase, when TeNT catalytic activity can still be detected (Mainardi *et al.*, 2012; Vannini *et al.*, 2016). In spite of the lengthening in active zone, we found a reduction in the fraction of released vesicles, suggesting that strengthening of inhibitory transmission may not be sufficient to counteract the unbalance produced by our experimental manipulation. Ultrastructural changes of release competent vesicles at excitatory synapses can only be detected at a later stage. In the chronic phase, we observed a reduction in docked release-competent vesicles consistent with a loss in spatial bias observed at excitatory synapses. Loss in spatial bias of release competent vesicles can be achieved pharmacologically by stabilising actin, leading to a slower release rate during 10 Hz stimulation (Marra et al., 2012). Our findings indicate that spatial organization of release-competent synaptic vesicles can be modulated *in vivo*. During the chronic phase, released glutamatergic vesicles are positioned farther away from the active zone, potentially to limit their re-use during high-frequency activity. This may homeostatically reduce the likelihood of generating spontaneous discharges in a hyperexcitable network. While a direct measure of the functional impact of this spatial reorganization is not yet possible, we can

speculate that the reduction of released vesicles at the active zone of excitatory synapses may fit with the models of occupancy and two-step release proposed over the years by the Marty's lab (Trigo *et al.*, 2012; Pulido *et al.*, 2015; Pulido and Marty, 2017; Miki *et al.*, 2018). Interpreted in the light of Marty's work, excitatory synapses in the chronic phase, although not changing in release fraction, may have a broader range of release latencies due to a reduction in occupancy at rest (Pulido *et al.*, 2015; Pulido and Marty, 2017; Miki *et al.*, 2018). Thus, in chronic epileptic mice the spatial organisation of release-competent vesicles farther from active zone may represent an attempt to homeostatically reduce networks' synchronicity without affecting the total number of vesicles released. While not sufficient to block seizures onset in TeNT epileptic model, this spatial rearrangement may account for the reported reduction of seizures observed in the chronic phase (27, 50). In an attempt to dissect the molecular mechanisms underlying this change in spatial bias, we performed an unbiased analysis of synaptosomes content in the two different phases of epilepsy. Unsurprisingly, we found upregulation of a number of proteins involved in DCV trafficking as expected during intense synaptic remodelling. We focussed our study on CPE and its effects on vesicular organization (Park, Cawley and Loh, 2008; Lou *et al.*, 2010). CPE is involved in many different pathways, including neuropeptides' synthesis and WNT/BDNF signalling, and it is known that regulates synaptic vesicles trafficking and positioning (Bamji *et al.*, 2006; Staras *et al.*, 2010; Skalka *et al.*, 2016). Interestingly, Lou et al. (2010) showed that hypothalamic synapses of CPE-KO mice have a marked reduction in docked vesicles and that the entire vesicular cluster is at a greater distance from the active zone; however, their readout did not allow discrimination between released and non-released vesicles. In line with these observations, we report a tightening of synaptic vesicle clusters, measured from the active zone, corresponding with elevated CPE expression (**Fig 3D, 3E**). It should be noted that our loss of spatial bias of recently released vesicles happens on a background of overall contraction of vesicular clusters. This observation offers a possible interpretation for the effect of CPE inhibition on epileptiform activity measured electrophysiologically *in vivo* (**Fig. 4**). It should be noted that the inhibition of CPE is likely to affect both active and resting vesicles. Further investigation in the specific role of release-competent vesicles in the chronic phase of epilepsy would require preferential manipulation of one of the two vesicular pools; unfortunately, to our knowledge, there are no pharmacological tools available for this purpose.

Our results indicate vesicular positioning as a novel site of modulation for homeostatic plasticity which may regulate high frequency discharges without affecting physiological neurotransmission. This modulation is a part of a much larger landscape of dynamic regulation of synaptic strengths following an experimental disruption of the balance between excitatory and inhibitory inputs.

Methods

Animals and TeNT injections

Adult (age > postnatal day 60) C57BL/6J mice used in this study were reared in a 12h light-dark cycle, with food and water available *ad libitum*. All experimental procedures were conducted in conformity with the European Communities Council Directive *n*◦ 86/609/EEC and were approved by the Italian Ministry of Health. TeNT injections were performed as previously described (Mainardi *et al.*, 2012; Vallone *et al.*, 2016; Vannini *et al.*, 2016, 2017).

206

207 FM 1-43FX injection and visual stimulation

208 Control and epileptic mice, deeply anesthetized with avertin (7 ml/kg; 20% solution in saline, i.p.;
209 Sigma Aldrich) and placed in a stereotaxic apparatus, received an injection of FM 1-43FX dye into the
210 primary visual cortex (i.e. 0.0 mm anteroposterior and 2.7 mm lateral to the lambda suture, 0.7 mm depth). 3
211 min later, animals were stimulated for 10 min with gratings and flashes (1 Hz, 0.06 c/deg, contrast 90%). All
212 visual stimuli were computer-generated on a display (Sony; 40 9 30 cm; mean luminance 15 cd/m2) by a
213 VSG card (Cambridge Research Systems). Mice, still under anaesthesia, were kept in the dark and perfused
214 through the heart with a fresh solution of 6% glutaraldehyde, 2% formaldehyde in PBS, as described in
215 (Jensen and Harris, 1989) right after the end of the visual stimulation. Brains were dissected, post-fixed for
216 2h and then placed into a 30% sucrose solution in PBS (Sigma Aldrich).

217

218 Photoconversion and Electron Microscopy analysis

219 All the following procedures were made in the dark. The protocol followed is described in detail in
220 (Marra *et al.*, 2014). Briefly, embedded in EPON, slices were collected with an ultramicrotome serial sections
221 (70 nm thickness) and placed in grids at RT. Thereafter, sections could be viewed with a transmission
222 electron microscope fitted with a cooled CCD camera. Images were acquired using local landmarks to
223 identify the same target synapse in consecutive sections and analysed using Image J/Fiji (NIH). At
224 ultrastructural level target synapses were randomly chosen and synaptic vesicles were scored based on their
225 vesicle luminal intensity using methods outlined previously (Darcy *et al.*, 2006), image names were changed
226 to ensure that the experimenters were blind to the experimental condition of each electron micrograph. A
227 terminal was considered inhibitory if at no spine or postsynaptic density could be observed in the middle
228 section and in least one of the adjecent sections. As expected (Meyer *et al.*, 2011; Tremblay, Lee and Rudy,
229 2016; van Versendaal and Levelt, 2016; Lim *et al.*, 2018), inhibitory terminals were estimated to be 15-25%
230 of the total.

231

232 Synaptosomes extraction and proteomic analysis

233 Synaptosomes were extracted using a slightly modified protocol taken from (Giordano *et al.*, 2018).
234 Visual cortices were gently homogenized in 500 ul of ice cold homogenizing buffer (0.32 M sucrose, 1 mM
235 EDTA, 1mg/ml BSA, 5 mM HEPES pH 7.4, proteases inhibitors) and centrifuged 10 min at 3000 g at 4°C;
236 supernatant was recovered and centrifuged again for 15 min at 14000 g at 4°C. After discarding supernatant,
237 the pelleted synaptosomes were suspended in 110 ul of Krebs-Ringer Buffer and 90 ul of Percoll (Sigma-
238 Aldrich) were added. A 2 min spin (14000 rpm, 4°C) was performed and enriched synaptosomes were
239 recovered from the surface of the solution with a P1000 tip and resuspended in 1ml of Krebs-Ringer buffer.
240 After an additional spin of 2 min (14000 rpm, 4°C), the supernatant was discarded and the pellet
241 resuspended in 20 ul of RIPA buffer.

242

243

244 Proteomics sample preparation and data analysis

245 Trypsin/LysC mix Mass Spec grade was purchased from Promega (Madison, WI). Tandem Mass
246 Tags (TMT 10-plex) kits and microBCA protein assay kit were purchased from Thermo Fisher Scientific

(Rockford, IL). All other reagents and solvents were purchased from Sigma-Aldrich (St. Louis, MO). Synaptosomes proteome extracts were quantified with a micro BCA protein assay and aliquots of 3.5 µg of proteins were diluted to 40 µL of RIPA/Trifluoroethanol (TFE) 50/50. Paramagnetic beads were added to each sample and further processed following a modified SP3 protocol for ultrasensitive proteomics as previously described (Pellegrini *et al.*, 2019). Synaptosomes proteins were reduced alkylated and digested with a mixture of trypsin/Lys-C (1:20 enzyme to protein ratio). Digested peptides were then quantified, and labeled with TMT 10-plex: samples were block randomized (www.sealedenvelope.com) over 5 TMT sets. Each TMT set included 2 normalization channels for batch corrections built pooling an aliquot from each digested synaptosome sample (Plubell *et al.*, 2017). TMT sets underwent high pH fractionation on an AssayMap Bravo (Agilent technologies) and fractions run on a nano-LC (Easy1000 Thermo Fisher Scientific) equipped with a 50 cm EasySpray column and coupled with an Orbitrap Fusion for MS3 analysis (Thermo Fisher Scientific). Experimental details regarding sample fractionation and LC-MS/MS runs have been already reported elsewere (Pellegrini *et al.*, 2019). Data were analysed using Proteome Discoverer 2.1. TMT data were normalized by internal reference scaling (Plubell *et al.*, 2017).

Electrophysiological recordings and drugs administration

Surgery was performed as described in (Spalletti *et al.*, 2017) but the small craniotomy was centered at 3 mm lateral to Lambda and performed in TeNT/RSA-injected hemisphere. Neuronal activity was recorded with a NeuroNexus Technologies 16-channel silicon probe with a single-shank (A1x16-3mm-50-177) mounted on a three-axis motorized micromanipulator and slowly lowered into the portion of visual cortex previously injected with TeNT or RSA solution at the depth of 1 mm. Before the beginning of the recording, the electrode was allowed to settle for about 10 min. Local Fiedl Potentials (LFP) signals were acquired at 40 kHz and bandpass filtered (30 Hz to 10 kHz) with a 16-channel Omniplex recording system (Plexon, Dallas, TX). Local Field Potentials (LFP) were computed online and referred to the ground electrode in the cerebellum. In order to verify whether interacting with Carboxypeptidase E (CPE) would change the number of seizures, we topically applied over the craniotomy 2- guanidinoethylmercaptosuccinic acid (GEMSA; Sigma-Aldrich) without removing the electrode. Neural signals were acquired at regular time intervals up to 30 min after GEMSA delivery to verify the effect and the penetration of the drug in the cortical layers. At the end of the experiment animals were sacrificed. Data were analysed offline with Offline Sorter and NeuroExplorer software (Plexon Inc, USA) and with custom made Python interfaces (Python.org). Movement artifacts were removed offline. The threshold for detecting epileptic spikes was set to 5 times the standard deviation of the LFP signal.

Statistical analysis

Statistical analysis was performed with Graph Pad (version 8) except for proteomics analysis, in which we used Perseus. Normality of distributions was assessed with D'Agostino test and appropriate test was chosen accordingly.

Acknowledgements

We thank Francesca Biondi (CNR Pisa) for the excellent animal care, Natalie Allcock and Ania Straatman-Iwanowska for the invaluable electron microscopy technical support and the scidraw.io team for the freely

available vector graphics used in Figures 1 and 4. During manuscript elaboration, EV was supported by a postdoctoral fellowship released by Fondazione Umberto Veronesi (Milan, Italy). This work was funded by Epilepsy Research UK (pilot grant PGE1501 and project grant P1802), Wellcome Trust Seed Award in Science (108201/Z/15/Z).

Declaration of interests

The authors declare no competing interests.

Author Contributions

E.V., M.C., V.M., L.MD conceived and designed the experiments; E.V., L.R., M.C. supplied the animal models; M.C., V.M. supervised the work; E.V., L.R., M.D., V.M. performed the experiments; E.V., M.D., V.M. analysed the data; E.V., V.M. wrote the paper. All authors contributed to critical revision of the manuscript.

FIGURE 1

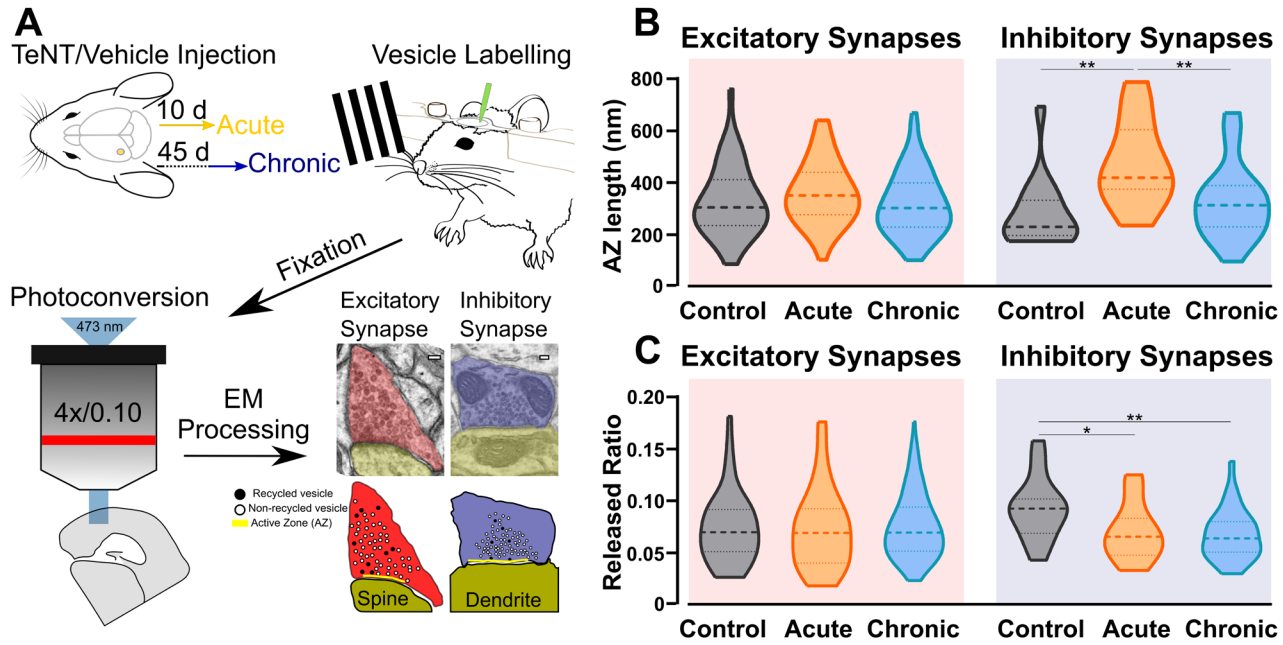

Figure 1: *Ultrastructural and functional changes at presynaptic terminals of TeNT-injected mice. **A**) Diagramatic labelling protocol. Visual cortices form mice in Control, Acute and Chronic groups were infused with FM1-43FX during mild visual stimulation. Brains were rapidly fixed and sliced to allow photoconversion of FM1-43FX signal before processing for electron microscopy. Individual presynaptic terminals were classified as excitatory (asymmetrical synapses, red) or inhibitory (symmetrical synapses, blue); size, position and numbers of active zone (AZ, yellow), non-released vesicles (open circles) and released vesicles (black circles) were analysed (scale bars 100nm). **B**) Left: Active zone (AZ) length in Control (grey), Acute (orange) and Chronic (blue) epileptic mice at excitatory synapses; no differences between the groups (Kruskal-Wallis test, p = 0.10). Distribution, median and quartiles shown for each group; Control n=41; Acute n=46; Chronic n=118. Right: Active zone (AZ) length in Control (grey), Acute (orange) and Chronic (blue) epileptic mice at inhibitory synapses (Kruskal-Wallis test, p < 0.01, Control vs Acute p<0.01, Control vs Chronic p>0.05, Chronic vs Acute p<0.01). Distribution, median and quartiles shown for each group; Control n=15; Acute n=14; Chronic n=29. **C**) Left: Released fraction of synaptic vesicles (labelled vesicles/total vesicles) in Control (grey), Acute (orange) and Chronic (blue) epileptic mice at excitatory synapses; no differences between the groups (Kruskal-Wallis test, p = 0.67). Distribution, median and quartiles shown for each group; Control n=47; Acute n=57; Chronic n=118. Right: Released fraction of synaptic vesicles of Control (grey), Acute (orange) and Chronic (blue) epileptic mice at inhibitory synapses. (Kruskal-Wallis test, p < 0.05, Control vs Acute p<0.05, Control vs Chronic p<0.01, Chronic vs Acute p>0.05). Distribution, median and quartiles shown for each group; Control n=16; Acute n=16; Chronic n=30.*

FIGURE 2

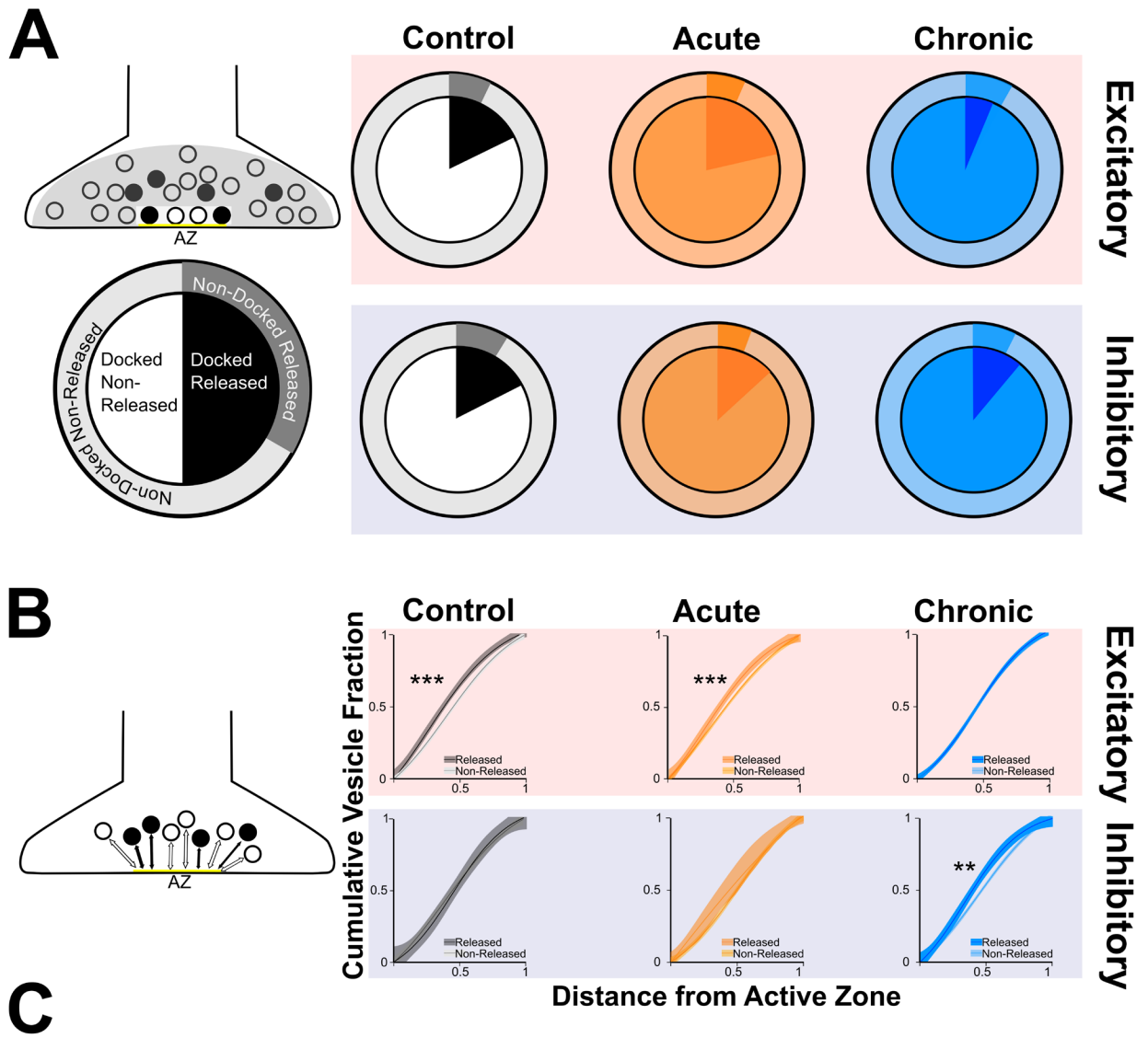

303

***Figure 2**: Changes in released vesicles' docking and spatial organization in chronic phase of epilepsy.* ***A**) Ratio of released vesicles in the docked and undocked population. Left: Diagram and legend for each pie chart. Top: Excitatory synapses' ratio of released vesicles (darker) in docked (inner pie chart) and undocked population (outer pie chart) in Control (grey), Acute (orange) and Chronic (blue) groups. Only the Chronic group shows a significant difference from expected frequencies based on control observation (Chi-squared test: p< 0.001). Bottom: Inhibitory synapses' ratio of released vesicles (darker) in docked (inner pie chart) and undocked population (outer pie chart) in control (grey), acute (orange) and chronic (blue) groups.* ***B**) Distance of released or non-released vesicles to the closest point on the active zone. Left: Diagram representing of how distance measures were taken at each synapse. Top: Sigmoid fit and 95% confidence interval of cumulative fraction of distance between released and not-released synaptic vesicles to the active zone at excitatory synapses in Control (grey), Acute (orange) and Chronic (blue) epileptic mice. Bottom: Sigmoid fit and 95% confidence interval of cumulative fraction of distance between released and not-released synaptic vesicles to the active zone at inhibitory synapses in Control (grey), Acute (orange) and Chronic (blue) epileptic mice. Paired t-test, Excitatory synapses: Control mice p = 0.0002 (n=40), Acute mice p = 0.0006 (n=41), Chronic mice p = 0.298 (n=112). Paired t-test, Inhibitory synapses: Control mice p = 0.06 (n=14), Acute mice p = 0.135 (n=13), Chronic mice p = 0.001 (n=28).* ***C**) 2D histograms of released vesicles distribution at excitatory (top) and inhibitory (bottom) synapses across the three conditions with active zone at the origin of the XY plane. Control (grey), Acute (orange) and Chronic (blue). Each synapse was spatially normalised (X and Y axes) and frequency is plotted on the Z axis. Scale bars: 0.1 normalised size X and Y; 0.1 fraction Z axis*

304

305

FIGURE 3

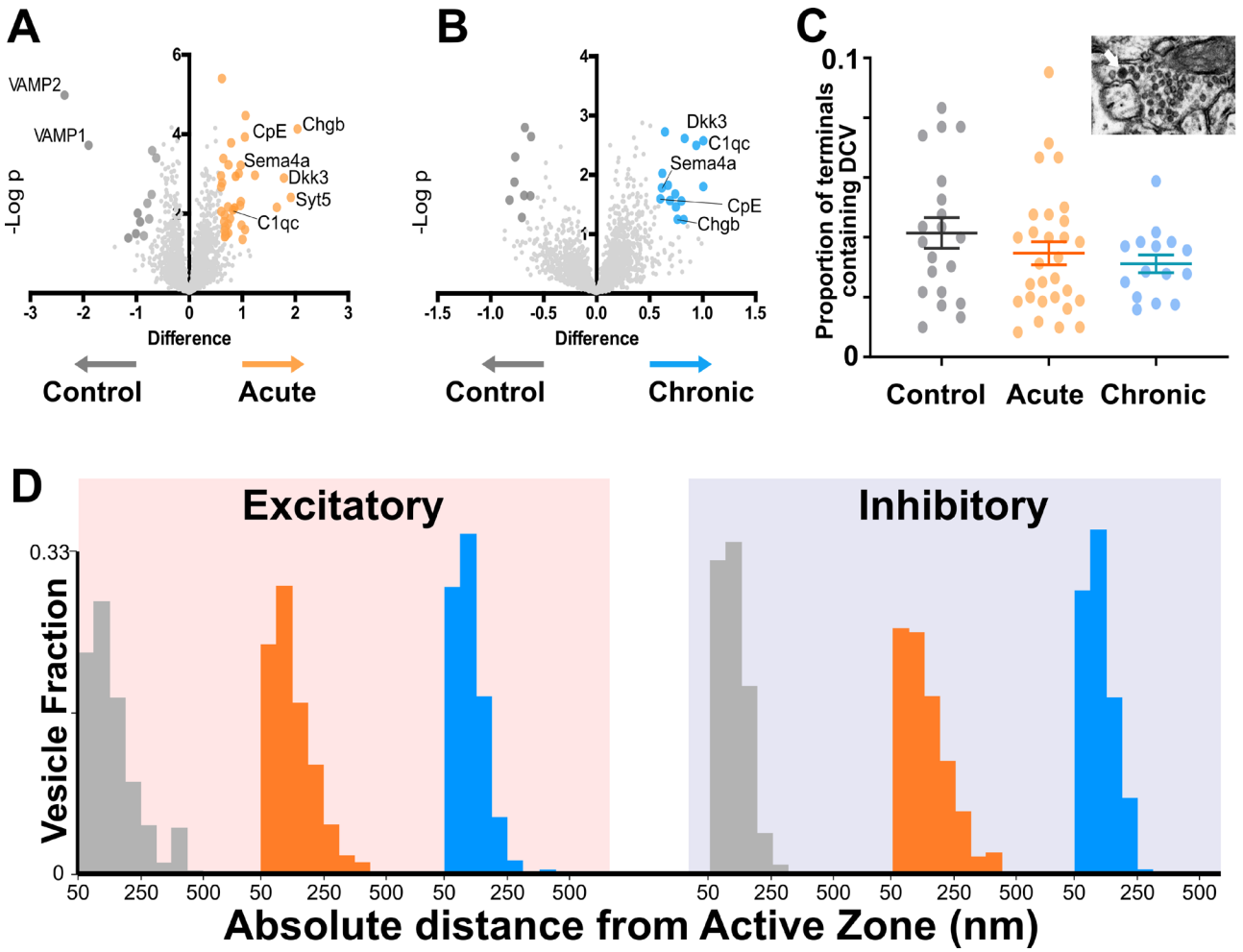

Figure 3: *Proteomics analysis of synaptosomes reveal an increase of proteins involved in vesicular positioning.*

A, B*) Differentially expressed proteins in Control vs Acute (**A**) and Chronic epileptic phase (**B**). Volcano plots are built plotting average ratio of TeNT vs. corresponding control against their t-test log P-values; significance thresholds: FDR > 0.05 and fold change > 0.6. Proteins significantly upregulated in Acute and Chronic tetanic animals are highlighted, respectively in orange and light blue; proteins significantly downregulated are in dark grey. Proteins abbreviations are Dkk3: Dickkopf-related protein 3; Sema4a: Semaphorin 4A; Cpe: carboxypeptidase e; Chgb: chromogranin b; Syt5: synaptotagmin5; VAMP1: Vesicle-associated membrane protein 1; VAMP2: Vesicle-associated membrane protein 2; C1qc: Complement C1q C Chain. **C)** Proportion of presynaptic terminals containing Dense Core Vesicles in different non-overlapping sampled areas of Control (grey; n=20), Acute (orange; n=29) and Chronic (blue; n=15) groups. No differences between groups (One Way ANOVA, p = 0.2869). Data are represented as mean ± SEM. Inset, a representative image of Dense Core Vesicles. **D)** Right: Distribution of distances of non-released vesicles from active zone at excitatory synapses in Chronic (grey; n=2140), Acute (orange; n=2503) and Chronic (blue; n=5705) groups (One-way ANOVA; F=238.15, p<0.0001, Control vs Actute: p<0.0001; Control vs Chronic: p<0.0001). Left: Distribution of distances of non-released vesicles from active zone at inhibitory synapses in Chronic (grey; n=543), Acute (orange; n=717) and Chronic (blue; n=1520) groups (F=75.57, p<0.0001, Control vs Actute: p<0.0001; Control vs Chronic: p>0.05).*

306

307

FIGURE 4

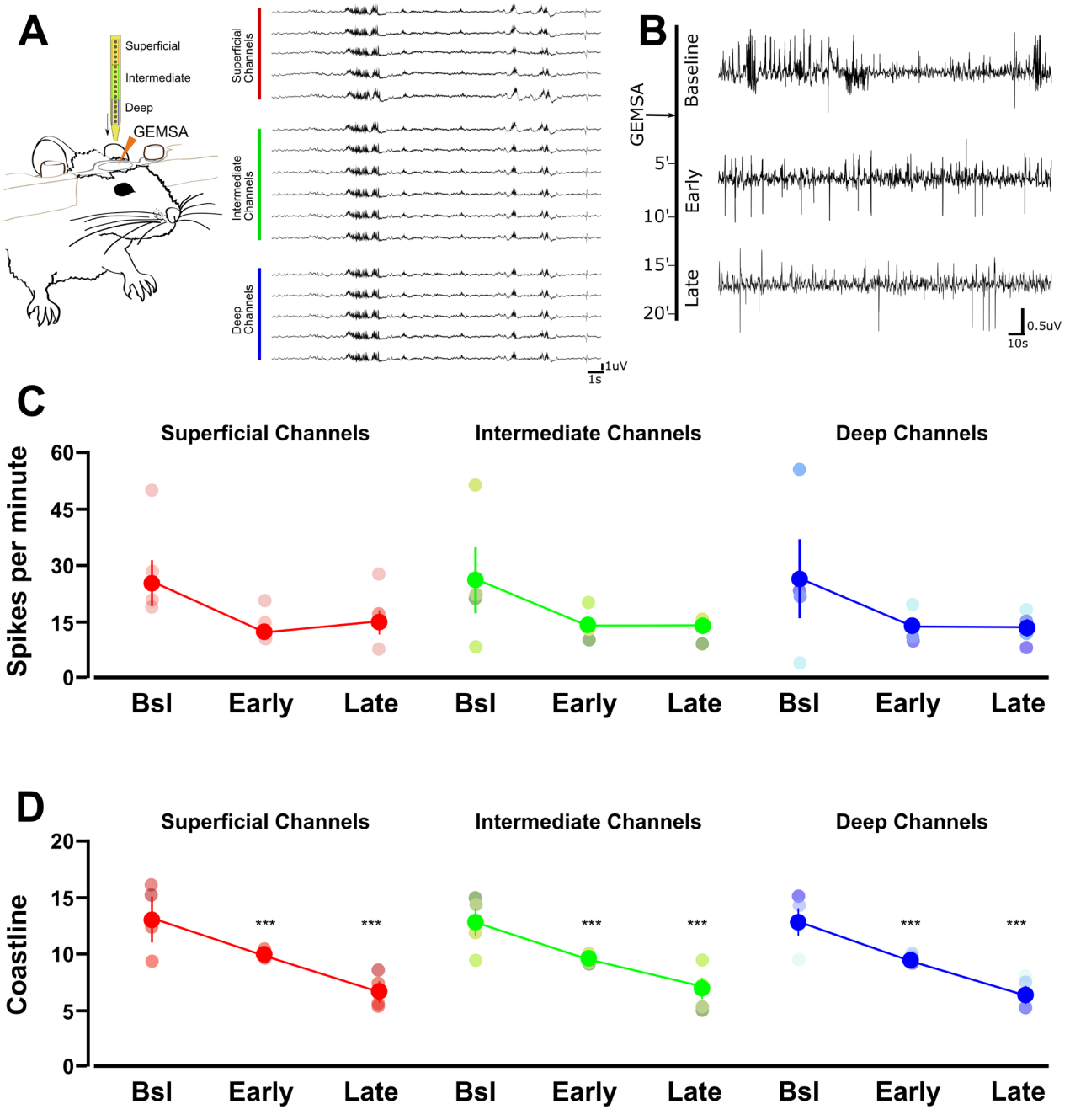

Figure 4: *Acute inhibition of Carboxypeptidase (CPE) decreases hyperexcitability in TeNT-injected mice.* ***A****) Diagram of experimental design, a 16-channel silicone probe was used to record LFP in different layers of the primary visual cortex, grouped channels were analysed in 3 groups according to their recording sites in relation to the surface of the cortex: the 5 most superficial, the 5 deepest and the 6 intermediate channels. GEMSA was applied locally to inhibit CPE activity.* ***B****) Examples of LFP traces obtained with a 16-channels probe from the visual cortex of an Acute epileptic mouse.* ***C****) LFP traces of an Acute epileptic mouse before (baseline, top) and after GEMSA administration at two different time points: early (5 to 10 minutes) and late (10 to 20 minutes).* ***D****) Number of multi-unit spikes recorded before (baseline) and after GEMSA administration at early and late time points. The analysis was differentially performed for superficial (left, red), intermediate (middle, green) and deep (right, blue) channels (Two-way ANOVA, did not detect any difference). The value of individual recordings are shown for each group.* ***E****) Coastline analysis of LFP signals recorded before (baseline) and after GEMSA administration at early and late time points. The analysis was differentially performed for*

superficial (left, red), intermediate (middle, green) and deep (right, blue) channels (Two-way ANOVA, Channel factor $p>0.05$, Time factor $p<0.001$; Baseline vs Early: $p < 0.01$, Baseline vs Late: $p < 0.001$, Early vs Late: $p < 0.001$, $n=4$). The mean, SEM and value of individual recordings are shown for each group.

References

Bamji, S. X. *et al.* (2006) 'BDNF mobilizes synaptic vesicles and enhances synapse formation by disrupting cadherin-β-catenin interactions', *Journal of Cell Biology*. doi: 10.1083/jcb.200601087.

Barnes, S. J. *et al.* (2015) 'Subnetwork-Specific Homeostatic Plasticity in Mouse Visual Cortex In Vivo', *Neuron*. Cell Press, 86(5), pp. 1290–1303. doi: 10.1016/j.neuron.2015.05.010.

Binda, P. *et al.* (2018) 'Response to short-term deprivation of the human adult visual cortex measured with 7T BOLD'. doi: 10.7554/eLife.40014.001.

Chang, B. L. *et al.* (2018) 'Semiology, clustering, periodicity and natural history of seizures in an experimental occipital cortical epilepsy model', *DMM Disease Models and Mechanisms*. doi: 10.1242/dmm.036194.

Cheng, Y., Cawley, N. X. and Loh, Y. P. (2014) 'Carboxypeptidase E (NF-α1): a new trophic factor in neuroprotection', *Neuroscience Bulletin*. Shanghai Institutes for Biological Sciences, Chinese Academy of Sciences, 30(4), pp. 692–696. doi: 10.1007/s12264-013-1430-z.

Clynen, E. *et al.* (2014) 'Neuropeptides as Targets for the Development of Anticonvulsant Drugs', *Molecular Neurobiology*. doi: 10.1007/s12035-014-8669-x.

Darcy, K. J. *et al.* (2006) 'Constitutive sharing of recycling synaptic vesicles between presynaptic boutons', *Nature Neuroscience*. doi: 10.1038/nn1640.

Davis, G. W. and Müller, M. (2015) 'Homeostatic Control of Presynaptic Neurotransmitter Release', *Annual Review of Physiology*. doi: 10.1146/annurev-physiol-021014-071740.

Desai, N. S. *et al.* (2002) 'Critical periods for experience-dependent synaptic scaling in visual cortex', *Nature Neuroscience*. doi: 10.1038/nn878.

Diering, G. H. *et al.* (2017) 'Homer1a drives homeostatic scaling-down of excitatory synapses during sleep', *Science*. doi: 10.1126/science.aai8355.

Dobolyi, A. *et al.* (2014) 'Receptors of Peptides as Therapeutic Targets in Epilepsy Research', *Current Medicinal Chemistry*. doi: 10.2174/09298673206613119154018.

Erchova, I. *et al.* (2017) 'Enhancement of visual cortex plasticity by dark exposure', *Philosophical Transactions of the Royal Society B: Biological Sciences*. Royal Society, 372(1715), p. 9. doi: 10.1098/rstb.2016.0159.

Ferecskó, A. S. *et al.* (2015) 'Structural and functional substrates of tetanus toxin in an animal model of temporal lobe epilepsy', *Brain Structure and Function*, 220(2), pp. 1013–1029. doi: 10.1007/s00429-013-0697-1.

Giordano, N. *et al.* (2018) 'Motor learning and metaplasticity in striatal neurons: Relevance for Parkinson's disease', *Brain*. doi: 10.1093/brain/awx351.

Gonzalez-Islas, C. *et al.* (2016) 'Tonic nicotinic transmission enhances spinal GABAergic presynaptic release and the frequency of spontaneous network activity', *Developmental Neurobiology*. doi: 10.1002/dneu.22315.

Gonzalez-Islas, C. and Wenner, P. (2006) 'Spontaneous network activity in the embryonic spinal cord regulates AMPAergic and GABAergic synaptic strength', *Neuron*. doi: 10.1016/j.neuron.2006.01.017.

González, O. C. *et al.* (2019) 'Ionic and synaptic mechanisms of seizure generation and epileptogenesis', *Neurobiology of Disease*. Academic Press Inc. doi: 10.1016/j.nbd.2019.104485.

Grubb, M. S. and Burrone, J. (2010) 'Activity-dependent relocation of the axon initial segment fine-tunes

neuronal excitability', *Nature*. doi: 10.1038/nature09160.

Harris, K. M. and Weinberg, R. J. (2012) 'Ultrastructure of synapses in the mammalian brain', *Cold Spring Harbor Perspectives in Biology*. doi: 10.1101/cshperspect.a005587.

Hengen, K. B. *et al.* (2013) 'Firing Rate Homeostasis in Visual Cortex of Freely Behaving Rodents'. doi: 10.1016/j.neuron.2013.08.038.

Ibata, K., Sun, Q. and Turrigiano, G. G. (2008) 'Rapid Synaptic Scaling Induced by Changes in Postsynaptic Firing', *Neuron*. doi: 10.1016/j.neuron.2008.02.031.

Jensen, F. E. and Harris, K. M. (1989) 'Preservation of neuronal ultrastructure in hippocampal slices using rapid microwave-enhanced fixation', *Journal of Neuroscience Methods*. doi: 10.1016/0165-0270(89)90146-5.

Keck, T. *et al.* (2011) 'Loss of sensory input causes rapid structural changes of inhibitory neurons in adult mouse visual cortex', *Neuron*. doi: 10.1016/j.neuron.2011.06.034.

Kovac, S. and Walker, M. C. (2013) 'Neuropeptides in epilepsy', *Neuropeptides*. doi: 10.1016/j.npep.2013.10.015.

Lim, L. *et al.* (2018) 'Development and Functional Diversification of Cortical Interneurons', *Neuron*. doi: 10.1016/j.neuron.2018.10.009.

Lou, H. *et al.* (2010) 'Carboxypeptidase E cytoplasmic tail mediates localization of synaptic vesicles to the pre-active zone in hypothalamic pre-synaptic terminals', *Journal of Neurochemistry*. John Wiley & Sons, Ltd (10.1111), 114(3), pp. 886–896. doi: 10.1111/j.1471-4159.2010.06820.x.

Lunghi, C. *et al.* (2015) 'Short-Term monocular deprivation alters GABA in the adult human visual cortex', *Current Biology*. Cell Press, 25(11), pp. 1496–1501. doi: 10.1016/j.cub.2015.04.021.

Lunghi, C., Burr, D. C. and Morrone, C. (2011) 'Brief periods of monocular deprivation disrupt ocular balance in human adult visual cortex'. doi: 10.1016/j.cub.2011.06.004.

Ma, T. *et al.* (2019) 'D-Serine Contributes to Seizure Development via ERK Signaling', *Frontiers in Neuroscience*. doi: 10.3389/fnins.2019.00254.

Maffei, A. *et al.* (2006) 'Potentiation of cortical inhibition by visual deprivation', *Nature*. doi: 10.1038/nature05079.

Maffei, A. and Turrigiano, G. (2008) 'Chapter 12 The age of plasticity: Developmental regulation of synaptic plasticity in neocortical microcircuits', *Progress in Brain Research*. doi: 10.1016/S0079-6123(07)00012-X.

Mainardi, M. *et al.* (2012) 'Tetanus neurotoxin-induced epilepsy in mouse visual cortex', *Epilepsia*, 53(7), pp. 132–136. doi: 10.1111/j.1528-1167.2012.03510.x.

Marra, V. *et al.* (2012) 'A Preferentially Segregated Recycling Vesicle Pool of Limited Size Supports Neurotransmission in Native Central Synapses', *Neuron*, 76(3), pp. 579–589. doi: 10.1016/j.neuron.2012.08.042.

Marra, V. *et al.* (2014) 'Ultrastructural readout of functional synaptic vesicle pools in hippocampal slices based on FM dye labeling and photoconversion', *Nature Protocols*, 9(6), pp. 1337–1347. doi: 10.1038/nprot.2014.088.

Meier, J. *et al.* (2014) 'Presynaptic mechanisms of neuronal plasticity and their role in epilepsy', *Frontiers in Cellular Neuroscience*. doi: 10.3389/fncel.2014.00164.

Meyer, H. S. *et al.* (2011) 'Inhibitory interneurons in a cortical column form hot zones of inhibition in layers 2 and 5A', *Proceedings of the National Academy of Sciences of the United States of America*. doi: 10.1073/pnas.1113648108.

Miki, T. *et al.* (2018) 'Two-component latency distributions indicate two-step vesicular release at simple glutamatergic synapses', *Nature Communications*. doi: 10.1038/s41467-018-06336-5.

Mrsic-Flogel, T. D. *et al.* (no date) 'Article Homeostatic Regulation of Eye-Specific Responses in Visual Cortex during Ocular Dominance Plasticity'. doi: 10.1016/j.neuron.2007.05.028.

Nikitidou Ledri, L. *et al.* (2016) 'Translational approach for gene therapy in epilepsy: Model system and unilateral overexpression of neuropeptide Y and Y2 receptors', *Neurobiology of Disease*. Academic Press Inc., 86, pp. 52–61. doi: 10.1016/j.nbd.2015.11.014.

Nilsen, K. E., Walker, M. C. and Cock, H. R. (2005) 'Characterization of the tetanus toxin model of refractory focal neocortical epilepsy in the rat', *Epilepsia*. doi: 10.1111/j.0013-9580.2005.26004.x.

De Paola, V. *et al.* (2006) 'Cell type-specific structural plasticity of axonal branches and boutons in the adult neocortex', *Neuron*. doi: 10.1016/j.neuron.2006.02.017.

Park, J. J., Cawley, N. X. and Loh, Y. P. (2008) 'Carboxypeptidase E Cytoplasmic Tail-Driven Vesicle Transport Is Key for Activity-Dependent Secretion of Peptide Hormones', *Molecular Endocrinology*. Narnia, 22(4), pp. 989–1005. doi: 10.1210/me.2007-0473.

Pellegrini, D. *et al.* (2019) 'Quantitative microproteomics based characterization of the central and peripheral nervous system of a mouse model of Krabbe disease', *Molecular and Cellular Proteomics*. doi: 10.1074/mcp.RA118.001267.

Plubell, D. L. *et al.* (2017) 'Extended multiplexing of tandem mass tags (TMT) labeling reveals age and high fat diet specific proteome changes in mouse epididymal adipose tissue', *Molecular and Cellular Proteomics*. doi: 10.1074/mcp.M116.065524.

Pulido, C. *et al.* (2015) 'Vesicular Release Statistics and Unitary Postsynaptic Current at Single GABAergic Synapses', *Neuron*. doi: 10.1016/j.neuron.2014.12.006.

Pulido, C. and Marty, A. (2017) 'Quantal fluctuations in central mammalian synapses: Functional role of vesicular docking sites', *Physiological Reviews*. doi: 10.1152/physrev.00032.2016.

Restani, L. *et al.* (2009) 'Functional Masking of Deprived Eye Responses by Callosal Input during Ocular Dominance Plasticity', *Neuron*. doi: 10.1016/j.neuron.2009.10.019.

Schiavo, G., Matteoli, M. and Montecucco, C. (2000) 'Neurotoxins affecting neuroexocytosis', *Physiological Reviews*. doi: 10.1152/physrev.2000.80.2.717.

Skalka, N. *et al.* (2016) 'Carboxypeptidase E (CPE) inhibits the secretion and activity of Wnt3a', *Oncogene*, 35, pp. 6416–6428. doi: 10.1038/onc.2016.173.

Snowball, A. *et al.* (2019) 'Epilepsy gene therapy using an engineered potassium channel', *Journal of Neuroscience*. doi: 10.1523/JNEUROSCI.1143-18.2019.

Spalletti, C. *et al.* (2017) 'Combining robotic training and inactivation of the healthy hemisphere restores pre-stroke motor patterns in mice', *eLife*. doi: 10.7554/eLife.28662.

Staras, K. *et al.* (2010) 'A Vesicle Superpool Spans Multiple Presynaptic Terminals in Hippocampal Neurons', *Neuron*, 66(1), pp. 37–44. doi: 10.1016/j.neuron.2010.03.020.

Stettler, D. D. *et al.* (2006) 'Axons and synaptic boutons are highly dynamic in adult visual cortex', *Neuron*. doi: 10.1016/j.neuron.2006.02.018.

Swann, J. W. and Rho, J. M. (2014) 'How is homeostatic plasticity important in epilepsy?', *Advances in Experimental Medicine and Biology*. doi: 10.1007/978-94-17-8914-1_10.

Tatavarty, V., Sun, Q. and Turrigiano, G. G. (2013) 'How to scale down postsynaptic strength', *Journal of*

Neuroscience. doi: 10.1523/JNEUROSCI.1676-13.2013.

Tremblay, R., Lee, S. and Rudy, B. (2016) 'GABAergic Interneurons in the Neocortex: From Cellular Properties to Circuits', *Neuron*. doi: 10.1016/j.neuron.2016.06.033.

Trigo, F. F. *et al.* (2012) 'Readily releasable pool of synaptic vesicles measured at single synaptic contacts', *Proceedings of the National Academy of Sciences of the United States of America*. doi: 10.1073/pnas.1209798109.

Turrigiano, G. (2012) 'Homeostatic synaptic plasticity: Local and global mechanisms for stabilizing neuronal function', *Cold Spring Harbor Perspectives in Biology*. doi: 10.1101/cshperspect.a005736.

Turrigiano, G. G. (2008) 'The Self-Tuning Neuron: Synaptic Scaling of Excitatory Synapses', *Cell*. doi: 10.1016/j.cell.2008.10.008.

Vallone, F. *et al.* (2016) 'Time evolution of interhemispheric coupling in a model of focal neocortical epilepsy in mice', *Physical Review E*, 94(3), p. 032409. doi: 10.1103/PhysRevE.94.032409.

Vannini, E. *et al.* (2016) 'Altered sensory processing and dendritic remodeling in hyperexcitable visual cortical networks', *Brain Structure and Function*. Springer Berlin Heidelberg, 221(6), pp. 2919–2936. doi: 10.1007/s00429-015-1080-1.

Vannini, E. *et al.* (2017) 'Dynamical properties of LFPs from mice with unilateral injection of TeNT', *BioSystems*. Elsevier Ireland Ltd, 161, pp. 57–66. doi: 10.1016/j.biosystems.2017.09.009.

van Versendaal, D. and Levelt, C. N. (2016) 'Inhibitory interneurons in visual cortical plasticity', *Cellular and Molecular Life Sciences*. doi: 10.1007/s00018-016-2264-4.

Vezzani, A. and Sperk, G. (2004) 'Overexpression of NPY and Y2 receptors in epileptic brain tissue: An endogenous neuroprotective mechanism in temporal lobe epilepsy?', *Neuropeptides*. doi: 10.1016/j.npep.2004.05.004.

Wefelmeyer, W., Puhl, C. J. and Burrone, J. (2016) 'Homeostatic Plasticity of Subcellular Neuronal Structures: From Inputs to Outputs', *Trends in Neurosciences*. doi: 10.1016/j.tins.2016.08.004.

Yamahachi, H. *et al.* (2009) 'Rapid Axonal Sprouting and Pruning Accompany Functional Reorganization in Primary Visual Cortex', *Neuron*. doi: 10.1016/j.neuron.2009.11.026.